Cite this: *INEOS OPEN*, **2020**, *3 (4)*, 150–155
DOI: 10.32931/io2019a

Received 13 June 2020,
Accepted 3 August 2020

http://ineosopen.org

ENVIRONMENTALLY FRIENDLY PREPARATION OF MAGNETIC COMPOSITES FEATURING PROTEOLYTIC PROPERTIES

N. A. Samoilova*

Nesmeyanov Institute of Organoelement Compounds, Russian Academy of Sciences, ul. Vavilova 28, Moscow, 119991 Russia

Abstract

The enzyme-containing magnetic composites are presented. The magnetic matrix for enzyme immobilization is obtained by sequential application of an amine-containing polysaccharide—chitosan and a synthetic polymer—poly(ethylene-*alt*-maleic acid) to the magnetite microparticles to form the interpolyelectrolyte complex shell. Then, the enzyme (trypsin) is immobilized by covalent or noncovalent binding. Thus, the suggested composites can be readily obtained in the environmentally friendly manner. The enzyme capacity of the resulting composites reaches 28.0–32.6 mg/g. The maximum hydrolysis rates of the H-Val-Leu-Lys-pNA substrate provided by these composites range within $0.60 \cdot 10^{-7}$–$0.77 \cdot 10^{-7}$ M/min.

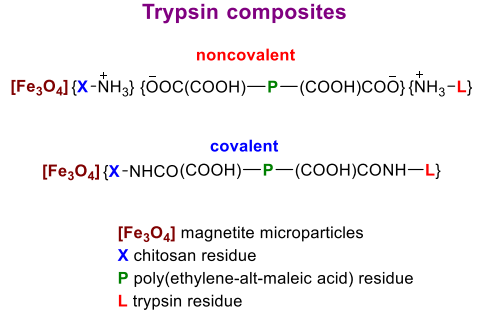

Key words: magnetic composites, interpolyelectrolyte complex, trypsin immobilization.

Introduction

Biocatalysis has emerged as one of the most promising technologies that enable green synthesis or hydrolysis of important chemicals and biologically active compounds for both the identification and manufacture of active pharmaceutical ingredients. Owing to recent advances in protein engineering, the number of biomolecules that can be synthesized and hydrolyzed using enzymes is steadily increasing. The immobilization of enzymes offers a range of advantages over the application of native enzymes, including the possibility of repeated use, stability during long-term operation and storage, ease of separation of enzymes from the reaction products, and reduced operational costs. Many new strategies for obtaining immobilized enzymes have been developed in recent years [1–10].

There are many methods for enzyme immobilization but the industry prefers simple and low-cost approaches. The most common methods are carrier-related technologies that utilize natural or synthetic polymers. The most popular methods are those based on noncovalent physical (adsorption or physical entrapment) or chemical (covalent binding and cross-linking) immobilization [10]. In noncovalent immobilization, an enzyme is adsorbed on a carrier and, thus, interacts with the matrix surface through ionic, hydrogen or hydrophobic bonds and van der Waals interaction. In this case, the protein is not denatured since the immobilization does not require activation stages and coupling agents. This is a cheap and simple method that usually provides high yields of immobilization [8, 11]. A covalent bond is usually formed between a functional group of the carrier matrix and a functional group of the enzyme that contains amino acid residues. The binding between the enzyme and the substrate material can be achieved either through the direct coupling of the corresponding functional groups, usually after activation of carboxyl groups, or through spacer groups [1, 10, 12].

Proteolytic enzymes, including serine proteases, are widely used in biotechnology, food production, and medicine for therapeutic, industrial or fundamental research. Their application scope includes, for example, peptide synthesis, preparation of recombinant antibody fragments for research, digestion of unwanted proteins during nucleic acid purification, removal of affinity tags from fusion proteins in recombinant protein techniques, and peptide sequencing [13–17]. One of the most commonly used enzyme for these purposes is trypsin and its immobilized forms. Trypsin is a proteolytic enzyme (highly specific endopeptidase) that is restricted to the positively charged lysine and arginine side chains. The cleavage occurs at the C-termini of these amino acids. The enzyme also hydrolyzes amide and ester linkages of synthetic derivatives of Lys and Arg. The active site of trypsin includes amino acid residues His46 and Ser183. The immobilization suitable for enzyme stabilization and reutilization prevents autolysis of the enzyme and may lead to lower process costs [18]. The methods for trypsin immobilization on the following organic substrates were reported: chitosan nanoparticles [19], chitosan nonwoven [20], poly(epoxy-acrylamide) cryogel [21], derivatized cellulose beads [22], and epoxy organic monoliths [23]. Fused silica capillary tubes were used as inorganic matrices for trypsin immobilization [24]. Trypsin was also immobilized on magnetic particles by cross-linking with glutaraldehyde [25] or magnetic nanoparticles by covalent binding with ethyl-*N*-(3-dimethylaminopropyl)carbodiimide [26].

Most of the methods for trypsin immobilization involve chemical activation of a matrix and/or the use of coupling agents. Earlier we suggested two reverse types of magnetic nano- and microparticles covered with interpolyelectrolyte complex shells bearing different functional groups in the outer shell layer [27].

In this report, an environmentally friendly method for trypsin immobilization is suggested that includes: 1) sequential two-step application of oppositely charged polymers (chitosan and alternant maleic acid copolymer) on the core of Fe_3O_4 microparticles (MMPs) and 2) noncovalent or covalent immobilization of trypsin. All the processes are realized under mild conditions without the use of toxic reagents and solvents.

Results and discussion

The surface-functionalized magnetic materials were prepared for the enzyme immobilization. Noncovalent (**1**) and covalent (**2**) trypsin-containing composites were synthesized (Scheme 1). An efficient technology for the preparation of carboxyl-functionalized magnetite microparticles, applicable for the enzyme immobilization, was developed based on the formation of a magnetite interpolyelectrolyte shell followed by its transformation. This was accomplished in two steps by the application of the following oppositely charged polymers to the magnetite particles: chitosan (CS) and maleic acid copolymer, namely, poly(ethylene-*alt*-maleic acid) (EM). The microparticle fraction was chosen because of the faster precipitation in the constant magnetic field compared to the nanoparticle fraction. The interpolyelectrolyte shell was constructed in an aqueous medium at room temperature. In our case, the carboxyl groups appeared to be on the surface of the microparticles and, thus, can be directly involved in enzyme immobilization by the Coulomb interaction of the corresponding functional groups or by the covalent binding of the enzyme after thermal activation of the composite.

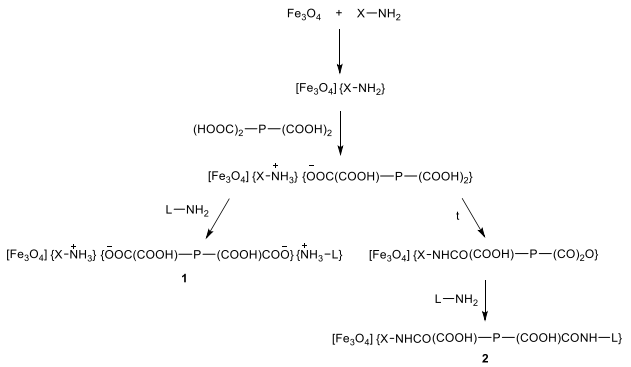

Scheme 1. Preparation of the magnetic composites (noncovalent (**1**) and covalent (**2**) trypsin composites). [Fe_3O_4] magnetite microparticles; X-NH_2, X-NH_3^+, and X-NH chitosan and chitosan residues; $(COOH)_2$-P-$(COOH)_2$, COO^-(COOH)-P-(COOH)COO^-, and -CO(COOH)-P-$(CO)_2O$ poly(ethylene-*alt*-maleic acid anhydride) residues; L-NH_2, NH_3^+-L, -NH-L trypsin and trypsin residues.

A structure of the interpolyelectrolyte shell is shown in Scheme 2. The chain structures of both interacting polymers are characterized by *trans*-alternation of monosaccharide residues in chitosan or dimer residues in the copolymer. The specific feature of the structure of the interpolyelectrolyte magnetite shell formed by the polysaccharide and copolymer in use is that, theoretically, half of the maleic acid units can take part in the interaction with the chitosan amino groups, and the rest of these units can be available for the interaction with the enzyme (a stoichiometric interpolyelectrolyte complex model that takes into account the distance between the interacting units was calculated using a HyperChem program). But the real structure of the polymer molecules in solution is sensitive to the solvent, temperature, ionic strength, and pH and is often aggregated. Thus, the interpolyelectrolyte shell really contained 25 wt % of CS and 1.8 wt % of EM. For the Fe_3O_4/CS/EM MMPs, we revealed 12.4 μmol/g of maleic acid residues which were not involved in the interpolyelectrolyte interaction and could be used for the modification (established by titration with methylene blue [27]).

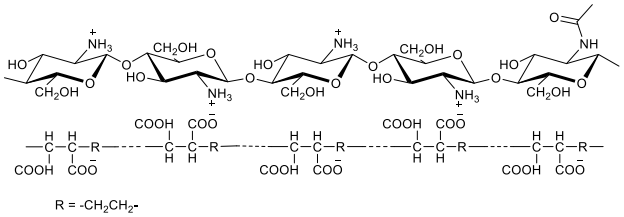

Scheme 2. Structure of the magnetite interpolyelectrolyte shell.

The saturation magnetization of Fe_3O_4/CS/EM was found to be 46 emu·g^{-1}. Transmission electron microscopy (TEM) was used to study the magnetite (Fig. 1) and magnetite–polymer composite (Fig. 2) particles. The average size of the composite particles ranged within 4–7 μm (Fig. 2a; standard deviation 3 μm). The image of these particles in the magnetic field is presented in Fig. 3. It is obvious that, in the field of a permanent magnet, the composite particles acquired an ordered structure.

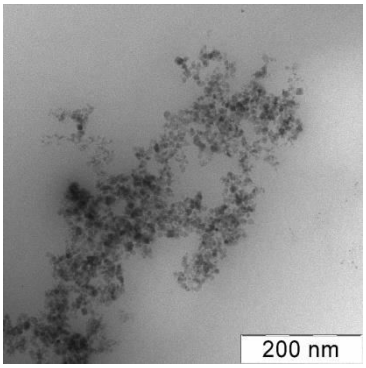

Figure 1. TEM micrograph of the magnetite particles.

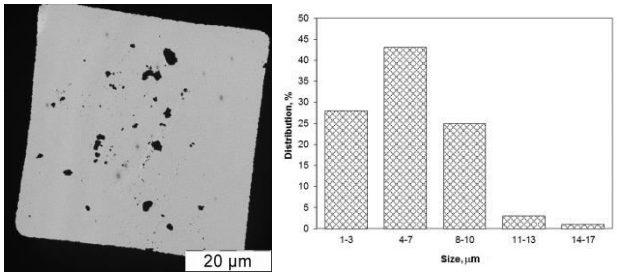

Figure 2. TEM micrograph of the magnetite particles covered by the interpolyelectrolyte shell.

Figure 3. Magnetic composite particles in the magnetic field (optical microscopy micrograph (×10)).

Figure 4 shows the FT-IR spectra of the magnetite particles with the CS, interpolyelectrolyte complex, and activated shells. In all the spectra the peaks at ν = 585–588 cm^{-1} were assigned to the characteristic Fe–O bond vibrations. The spectrum of the Fe_3O_4/CS particles (Fig. 4, *1*) shows the characteristic absorption bands at 3400–3200 cm^{-1} that can be assigned to the OH and NH stretching vibrations. The following vibrations were also observed: 2921, 2871 cm^{-1} (CH); 1071 cm^{-1} (C–O–C); 1649 cm^{-1} (amide I); 1554, 1599 cm^{-1} (amide II); and 1377 cm^{-1} (CH_3) (CH_3CONH groups of CS). The spectrum of Fe_3O_4/CS/EM (Fig. 4, *2*) shows the absorption bands in the range of 1632–1708 cm^{-1}, ν_{COO} = 1555, 1400 cm^{-1}, and ν_{C-O} = 1074 cm^{-1}, which refer to the CS/EM interpolyelectrolyte complex. The thermal treatment of the composite (Fig. 4, *3*) led to the cross-linking of the CS/EM shell and gave rise to the absorption bands of amide groups at 1549 cm^{-1} and $\nu_{C=O}$ at 1710 cm^{-1} and 1776 cm^{-1}. The last two bands indicate the appearance of a cyclic structure of succinic anhydride.

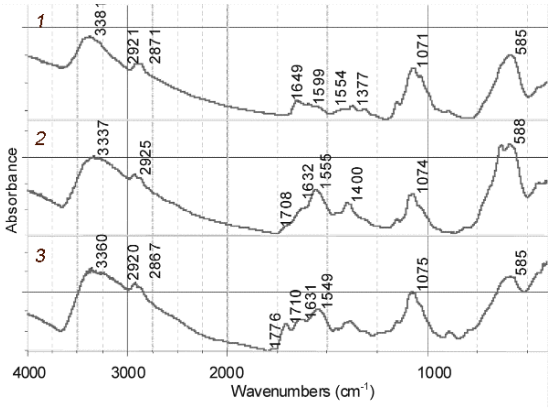

Figure 4. FT-IR spectra of the magnetite composites: Fe_3O_4/CS (*1*), Fe_3O_4/CS/EM (*2*), Fe_3O_4/CS/EM after thermal treatment (*3*).

The immobilization of trypsin was carried out in two ways to obtain the noncovalent and covalent composites: by the direct mixing of the components or by the introduction of the enzyme into the preactivated matrix. The reactivity of the resulting anhydride groups of MMPs ensured the binding of trypsin through the amide bonds under mild conditions in an aqueous medium without the use of coupling agents. The Fe_3O_4/CS/EM particles were activated by heating for covalent enzyme immobilization. It is well known that trypsin contains a significant number of positively charged amino acid residues that can bind with the negatively charged or activated matrix [28].

In this case, the amino acid residues, being a part of the enzyme active center (His and Ser), cannot be involved in the interaction with the matrix. The presence of the polymer carboxyl groups in the microenvironment of trypsin should contribute to its activity and stability since trypsin is more stable in the acidic medium [29].

The loading capacity of the stabilized enzyme–matrix catalytic system is presented in Table 1.

Table 1. Composition and properties of the resulting magnetic composites

Sample	Trypsin binding capacity of the composites		
	Calculated[a] (μmol/g)	Found	
		μmol/g	mg/g
Noncovalent composite	12	1.4	32.6
Covalent composite	12	1.2	28.0

[a] the content of dicarboxylic acid (anhydride) residues on the surface of the composite particles calculated according to Ref. [27].

The data obtained suggest that approximately 10 dicarboxylic acid residues available for binding in the composite account for 1 binding enzyme molecule, which is likely to be dictated by the steric features of the introduced object. The amount of the enzyme introduced into the composite by the described immobilization methods was about 30 mg/g. It should be noted that, as in the case of the covalent binding, the noncovalent binding of trypsin results in strong multicenter polyfunctional enzyme binding. Free trypsin was washed from the composite with a salt and buffer solution. Earlier we have shown that the maleic anhydride groups of the corresponding copolymers easily react in water with the primary glycine amino groups of glycyl-spaced carbohydrate, N-Gly-3'-sialyllactose, in one step *via* formation of the amide bonds without the use of coupling agents. The resulting glycoconjugate contains 14–15 mol % of carbohydrates [30]. The specific activity of the trypsin composites was studied towards two different substrates: amino acid derivative L-Arg-2-naphthylamide·HCl (R-NPA) and peptide H-Val-Leu-Lys-pNA·HCl (VLK-NA). Table 2 presents the data on the conversion of these substrates under the action of the composites obtained. It is obvious that, in the case of the covalent composite, the enzymatic activity of trypsin is somewhat lower than in the case of the noncovalently bound enzyme, presumably, due to the closer contact with the matrix. The structural features of the substrates are also of great importance [31].

Taking into account almost the same concentrations of the substrates in the reaction media and close enzyme/substrate ratios, it can be concluded that the naphthylamide moiety is cleaved from the amino acid substrate worse than the nitroanilide unit from the peptide substrate. This may be caused by a greater steric hindrance associated with the elimination of the larger amine moiety—naphthylamine. This trend was also observed with the native enzyme. The presence of calcium cations in the system slightly increased the activity of the enzyme as was shown earlier [32].

It should also be noted that, both in the case of noncovalent and covalent binding, the enzyme is firmly fixed in the matrix

Table 2. Degree of conversion of the substrates under the action of the trypsin composites during the first 30 min

Sample	Degree of substrate conversion, %	
	R-NPA	VLK-NA
Trypsin	57.0[a]	70.0[b]
Noncovalent composite	36.3[c]	75.0[d]
Noncovalent composite/Ca^{2+}	39.4[c]	–
Covalent composite	31.5[c]	76.1[d]
Covalent composite/Ca^{2+}	39.0[c]	–

[a] trypsin concentration $6.4\cdot10^{-6}$ M; substrate initial concentration $4.7\cdot10^{-5}$ M;
[b] trypsin concentration $4.8\cdot10^{-6}$ M; substrate initial concentration $7.0\cdot10^{-5}$ M;
[c] apparent trypsin concentration (calculated from the content of trypsin in the composite and solution volume) $9.5\cdot10^{-6}$ M; substrate initial concentration $1.4\cdot10^{-4}$ M;
[d] apparent trypsin concentration (calculated from the content of trypsin in the composite and solution volume) $5.1\cdot10^{-6}$ M; substrate initial concentration $6.0\cdot10^{-5}$ M.

and, after regeneration, this composite almost did not lose its activity.

All the composites obtained can be used repeatedly almost with no loss in the activity even in three cycles.

Figure 5 demonstrates the changes in the rates of enzymatic reactions with the amino acid substrate in the initial period of time. In less than 10 min from the reaction beginning, the optical density of a supernatant solution was not taken into account due to the possible interference as a result of incomplete precipitation of the composite upon application of a constant magnetic field. The rates of enzymatic reactions in 1 h noticeably decreased for all the systems under consideration. Of note is also the trend associated with a slightly higher rate of enzymatic hydrolysis in the case of the noncovalent composite compared to that for the covalent composite. Calcium salts of the enzyme-containing composites were also more effective. The maximum rate of hydrolysis of the H-Val-Leu-Lys-pNA peptide substrate was $0.60\cdot10^{-7}$ and $0.77\cdot10^{-7}$ M/min for the covalent and noncovalent samples, respectively. The sample with the noncovalent binding of the enzyme showed significant hydrolase activity but a possible drawback of this compound is the dependence of its stability on the operating conditions.

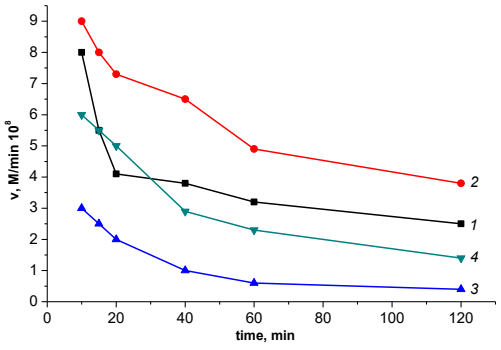

Figure 5. Rates of enzymatic reactions (v = dc/dt) with R-NPA: noncovalent trypsin composite (*1*), noncovalent composite/Ca^{2+} (*2*), covalent trypsin composite (*3*), covalent composite/Ca^{2+} (*4*).

The resulting composites are mechanically stable and practically nonporous, which reduces the steric hindrances. The composite samples can be isolated in the dry form and stored for several months without the loss of their properties.

Experimental

Materials

Poly(ethylene-*alt*-maleic anhydride) (Monsanto, USA, M = $2.5\cdot10^4$) was hydrolyzed to the corresponding copolymer of maleic acid by dissolving in deionized water followed by lyophilization. Chitosan (deacetylation degree 85%, M = $9.0\cdot10^4$) was purchased from Bioprogress (Russia). The following reagents were used without purification: $Fe_2(SO_4)_3\cdot9H_2O$, $FeSO_4\cdot12H_2O$, $NaHCO_3$, NaOH, TRIS, $CaCl_2$, NaCl, HCl (all of the analytical grade, Reakhim), bovine trypsin (Sigma-Aldrich), L-Arg-2-naphthylamide·HCl (R-NPA) (Serva), and H-Val-Leu-Lys-pNA·HCl (VLK-NA) (Bachem).

Methods

The compositions of the magnetite composites were determined based on the Fe, C, H, and N elemental analyses (Laboratory for Microanalysis, INEOS RAS).

The FT-IR spectra of MMPs were recorded using a Nicolet Magna IR-720 FT-IR spectrometer (USA). A BHV-55 vibrating sample magnetometer was used to characterize the magnetic saturations of MMPs. The UV-vis data were obtained with a UVIKON-922 (BRD) spectrophotometer. The transmission electron micrographs were obtained with a LEO 912 AB microscope (Omega, Karl Zeiss; BRD) operating at the accelerating voltage of 100 kV. For the TEM studies, a drop of the particle dispersion in water was placed onto a Formvar coated copper grid and then dried. The size distributions of the particles were obtained by measuring 100 individual particles. The optical microscopic studies were performed using an Eclise H550S (Nikon, Japan) microscope equipped with a Kodak DC 120 Digital Camera.

Syntheses

Preparation of the composite matrix. The magnetite particles were obtained by dehydration of freshly prepared Fe^{+2} and Fe^{+3} hydroxides derived from their salts (taken in 1:2 molar ratio) in an alkaline solution according to the published procedure [33]. $Fe_2(SO_4)_3\cdot9H_2O$ (1.4 g) and $FeSO_4\cdot12H_2O$ (0.7 g) were dissolved in deionized water (25 mL). Then, 25% solution of ammonia (10 mL) in water (40 mL) was added to the reaction mixture. The resulting mixture was sonicated (22 kHz) for 2 min. The black precipitate of magnetite was collected with the use of a permanent magnet (magnetic field strength 2000 G) and washed with deionized water several times until neutral pH of the effluent. The dispersion (1.6 g) contained approximately 20% of dry Fe_3O_4. The resulting particles were used as obtained or lyophilized.

The magnetite interpolyelectrolyte coating was prepared according to the published procedure [27]. The freshly prepared magnetite (1.0 g of the dispersion in deionized water containing 0.23 g of dry Fe_3O_4) was mixed with deionized water (50 mL) and sonicated (22 kHz) for 2 min. Then, 2% solution of chitosan (CS) in 1% aq. CH_3COOH (10 mL) was added. The reaction mixture was additionally sonicated for 2 min. The yield of Fe_3O_4/CS particles was 93%.

The content of chitosan in the shell of the Fe_3O_4/CS composite was calculated using the data of elemental analyses according to the following algorithm. The theoretical content of elements in the chitosan unit was calculated given that chitosan contains 15% of acetyl groups. Anal. Calcd. for $C_{6.3}H_{11.3}N_1O_{4.15}$: C, 45.2; H, 6.75; N, 8.37. Found for the Fe_3O_4/CS composite: Fe, 54.2; C, 11.8; H, 1.76; N, 2.40 (%). From the comparison of the results obtained for carbon and nitrogen in the composite with the values calculated for chitosan, it is obvious that chitosan content in the composite shell was 25.9 wt %.

Then, the Fe_3O_4/CS particles (0.20 g) were dispersed in deionized water (100 mL) and sonicated (22 kHz) for 2 min. After the addition of 2% aq. solution of poly(ethylene-*alt*-maleic acid) (EM) (pH = 5, 2 mL), the reaction mixture was sonicated for 2 min. The composites were collected with the use of a permanent magnet and washed with deionized water. The composite nanoparticles were separated from the microparticles (MMPs) by centrifugation at 3000 rpm for 5 min. The yield of MMPs after freeze drying was 0.21 ± 0.04 g. Found for the Fe_3O_4/CS/EM composite: Fe, 51.2; C, 12.2; H, 1.91; N, 2.10 (%). Based on the nitrogen content in this sample, the chitosan content calculated according to the above algorithm for the Fe_3O_4/CS was 25%. An increase in the content of carbon in the Fe_3O_4/CS/EM sample can be explained by the introduction of the polymer. Taking into account the molecular formula of the copolymer unit $C_6H_8O_4$, the comparison of the theoretical carbon content in the net polymer (50%) with and an increase in the carbon content in the sample (given the amount of carbon accounting for 25% of the chitosan content) affords the polymer content in the sample equal to 1.8 wt %.

Immobilization of trypsin. *Covalent immobilization of trypsin.* Before the enzyme immobilization, the following activation procedure and cross-linking of the magnetite interpolyelectrolyte shell of Fe_3O_4/CS/EM MMPs were carried out. A powdered composite sample was heated under vacuum over P_2O_5 at 110 °C for 3 h. After cooling to room temperature, the activated MMPs (50 mg) were added to trypsin (5 mg) in water (pH = 8, 3 mL) under vigorous stirring. The mixture was stirred at room temperature for 24 h. The magnetic particles were collected using a permanent magnet and washed sequentially with 1M KCl and deionized water until the absence of trypsin in the effluent (UV-vis absorption spectroscopic control at 280 nm). The contents of trypsin immobilized on the activated MMPs were calculated from a balance of the introduced enzyme and trypsin contained in the washing water taking into account the extinction of trypsin ($E^{0.1\%}$ = 1.54 (280 nm)) [34].

Non-covalent immobilization of trypsin. Non-covalent immobilization of trypsin was realized according to the above-described protocol without the matrix activation procedure.

Investigation of the catalytic properties of the resulting composites. The covalent or noncovalent composite (50 mg) in TBS buffer (5 mL; 50 mM, 0.15 M NaCl, pH = 7.4) was placed in a temperature-controlled cell heated to 25 °C followed by the addition of R-NPA (concentration in the solution $1.35 \cdot 10^{-4}$ M) or VLK-NA (concentration in the solution $6.10 \cdot 10^{-5}$ M). The reaction was carried out for 4 h. To study the effect of calcium cations on the course of the reaction, a solution of $CaCl_2$ ($1.8\ 10^{-2}$ M; 0.5 mL) was added to the system. The qualitative monitoring of the substrate hydrolysis was performed using UV-vis absorption spectroscopy by analyzing the supernatant probes after the collection of the enzyme-containing composite with a permanent magnet. For the R-NPA amino acid substrate, the monitoring was performed based on the extinction of 2-naphthylamine at 236 nm, log E = 4.76 [35], for the VLK-NA peptide substrate—based on the extinction of 4-nitroaniline at 410 nm, ε = 8270 $M^{-1}cm^{-1}$ (Serva). After the reaction completion, the enzyme-containing composite can be washed with a salt solution and deionized water and, then, either used the second time or, after dehydration with acetone, dried and stored.

Conclusions

A simple method for the formation of the magnetic matrix for enzyme immobilization was elaborated. The composites were obtained by applying the amine-containing polysaccharide and dicarboxylic acid bearing a synthetic polymer to the magnetite microparticles to form the interpolyelectrolyte complex shell followed by the introduction of the enzyme by ionic or covalent (after thermal activation of the magnetite shell) binding. The suggested composites can be readily obtained (without recourse to toxic solvents or coupling agents) and used (without filtration or centrifugation to separate the composite). The enzyme loading capacity of the composites reached 28.0–32.6 mg/g. The maximum hydrolysis rate of the H-Val-Leu-Lys-pNA substrate was $0.60 \cdot 10^{-7}$–$0.77 \cdot 10^{-7}$ M/min for the covalent and noncovalent samples, respectively. The sample with the noncovalently bound enzyme exhibited significant hydrolase activity but the composite stability depended on the operating conditions. The composite samples can be isolated in the dry form and stored for several months without the loss of properties.

The suggested method opens the way to successful immobilization of various amine-containing ligands or biologically active compounds to produce multienzyme systems. Subsequently, the composites can be endowed with various physical and chemical properties [36] and used in enzymatic synthesis as well as manufacture of mixtures for parenteral nutrition.

Acknowledgements

This work was performed with the financial support from the Ministry of Science and Higher Education of the Russian Federation using the equipment of the Center for Molecular Composition Studies of INEOS RAS.

The author is grateful to Dr. Z. S. Klemenkova for IR spectroscopic studies.

Corresponding author

* E-mail: samoilova@ineos.ac.ru

References

1. R. Fernandez-Lafuente, *Molecules*, **2019**, *24*, 4619. DOI: 10.3390/molecules24244619

2. P. N. Devine, R. M. Howard, R. Kumar, M. P. Thompson, M. D. Truppo, N. J. Turner, *Nat. Rev. Chem*., **2018**, *2*, 409–421. DOI: 10.1038/s41570-018-0055-1
3. Y. Zhu, Q. Chen, L. Shao, Y. Jia, X. Zhang, *React. Chem. Eng.*, **2020**, *5*, 9–32. DOI: 10.1039/C9RE00217K
4. M. Bilal, M. Asgher, H. Cheng, Y. Yan, H. M. N. Iqbal, *Crit. Rev. Biotechnol.*, **2019**, *39*, 202–219, DOI: 10.1080/07388551.2018.1531822
5. F. Shakerian, J. Zhao, S.-P. Li, *Chemosphere*, **2020**, *239*, 124716. DOI: 10.1016/j.chemosphere.2019.124716
6. A. Nathani, N. Vishnu, C. S. Sharma, *J. Electrochem. Soc.*, **2020**, *167*, 037520. DOI: 10.1149/2.0202003JES
7. X. Cai, M. Zhang, W. Wei, Y. Zhang, Z. Wang, J. Zheng, *Biotechnol. Lett*., **2020**, *42*, 269–276. DOI: 10.1007/s10529-019-02771-6
8. A. K. Khan, N. M. Mubarak, E. C. Abdullah, M. Khalid, S. Nizamuddin, H. A. Baloch, M. T. H. Siddiqui, *IOP Conf. Ser.: Mater. Sci. Eng.*, **2019**, *495*, 012055. DOI: 10.1088/1757-899X/495/1/012055
9. M. Koenig, U. König, K.-J. Eichhorn, M. Müller, M. Stamm, P. Uhlmann, *Front. Chem*., **2019**, *7*, 101. DOI: 10.3389/fchem.2019.00101
10. A. Basso, S. Serban, *Mol. Catal.*, **2019**, *479*, 110607. DOI: 10.1016/j.mcat.2019.110607
11. T. Jesionowski, J. Zdarta, B. Krajewska, *Adsorption*, **2014**, *20*, 801–821. DOI: 10.1007/s10450-014-9623-y
12. S. Nisha, S. Arun Karthick, N. Gobi, *Chem. Sci. Rev. Lett.*, **2012**, *1 (3)*, 148–155.
13. J. A. Mótyán, F. Tóth, J. Tőzsér, *Biomolecules*, **2013**, *3*, 923–942. DOI: 10.3390/biom3040923
14. R. Sawant, S. Nagendran, *World J. Pharm. Pharm. Sci*., **2014**, *3*, 568–579.
15. G. Hedayati, A. M. Sani, *Biotechnol.: Indian J*., **2016**, *12*, 18–24.
16. H. J. Klasen, *Burns*, **2000**, *26*, 207–222. DOI: 10.1016/s0305-4179(99)00117-5
17. M. Rosulek, P. Darebna, P. Pompach, L. Slavata, P. Novak, *Catalysts*, **2019**, *9*, 833. DOI: 10.3390/catal9100833
18. F. E. Regnier, J. H. Kim, *Bioanalysis*, **2014**, *6*, 2685–2698. DOI: 10.4155/bio.14.216
19. Z.-X. Tang, J.-Q. Dian, L.-E. Shi, *Process Biochem.*, **2006**, *41*, 1193–1197. DOI: 10.1016/j.procbio.2005.11.015
20. J. S. Kim, S. Lee, *Polymers*, **2019**, *11*, 1462. DOI: 10.3390/polym11091462
21. W. Johnson, Y. M. M. Makame, *Tanzania J. Sci.*, **2012**, *38*, 54–64.
22. V. G. Janolino, H. E. Swaisgood, *J. Food Biochem*., **2002**, *26*, 119–129. DOI: 10.1111/j.1745-4514.2002.tb00869.x
23. E. Calleri, C. Temporini, F. Gasparrini, P. Simone, C. Villani, A. Ciogli, G. Massolini, *J. Chromatogr. A*, **2011**, *1218*, 8937–8945. DOI: 10.1016/j.chroma.2011.05.059
24. K. Hata, Y. Izumi, T. Hara, M. Matsumoto, T. Bamba, *Anal. Chem.*, **2020**, *92*, 2997–3005. DOI: 10.1021/acs.analchem.9b03993
25. E. Van Leemputten, M. Horisberger, *Biotechnol. Bioeng*., **1974**, *16*, 385–396. DOI: 10.1002/bit.260160308
26. T.-H. Wang, W.-C. Lee, *Biotechnol. Bioprocess Eng.*, **2003**, *8,* 263–267. DOI: 10.1007/BF02942276
27. N. Samoilova, V. Tikhonov, M. Krayukhina, I. Yamskov, *J. Appl. Polym. Sci*., **2014**, *131*, 39663. DOI: 10.1002/APP.39663
28. Z. Wu, G. Jiang, N. Wang, J. Wang, S. Chen, Z. Xu, *Int. J. Pept. Res. Ther*., **2008**, *14*, 81. DOI: 10.1007/s10989-007-9108-x
29. *Advances in Enzymology and Related Areas of Molecular Biology*, V. 85, F. F. Nord (Ed.), Wiley, **2009**.
30. N. A. Samoilova, M. A. Krayukhina, D. A. Popov, N. M. Anuchina, V. E. Piskarev, *Biointerface Res. Appl. Chem*., **2018**, *8*, 3095–3099.
31. M. M. Nachlas, R. E. Plapinger, A. M. Seligman, *Arch. Biochem. Biophys*., **1964**, *108*, 266–274. DOI: 10.1016/0003-9861(64)90386-8
32. K. A. Walsh, *Methods Enzymol*., **1970**, *19*, 41–63. DOI: 10.1016/0076-6879(70)19006-9
33. W. C. Elmore, *Phys. Rev*., **1938**, *54*, 309–310. DOI: 10.1103/PhysRev.54.309
34. M. Tashiro, Y. Kihira, Y. Katayama, Z. Maki, *Agric. Biol. Chem*., **1989**, *53*, 443–451. DOI: 10.1271/bbb1961.53.443
35. *Handbook of Chemistry and Physics*, R. C. Weast (Ed.), CRC Press, Boca Raton, **1979**.
36. E. Yu. Kramarenko, G. V. Stepanov, A. R. Khokhlov, *INEOS OPEN*, **2019**, *2*, 178–184. DOI: 10.32931/io1926r